IRIS AperTO

UNIVERSITÀ DEGLI STUDI DI TORINO

AperTO - Archivio Istituzionale Open Access dell'Università di Torino

CSF1R Is Required for Differentiation and Migration of Langerhans Cells and Langerhans Cell Histiocytosis (*LONARDI S and SCUTERA S CO-FIRST AUTHORS)

This is a pre print version of the following article:

Original Citation:

Availability:

This version is available http://hdl.handle.net/2318/1741053 since 2020-07-21T16:58:23Z

Published version:

DOI:10.1158/2326-6066.CIR-19-0232

Terms of use:

Open Access

Anyone can freely access the full text of works made available as "Open Access". Works made available under a Creative Commons license can be used according to the terms and conditions of said license. Use of all other works requires consent of the right holder (author or publisher) if not exempted from copyright protection by the applicable law.

(Article begins on next page)

25 April 2024

CSF1R is required for differentiation and migration of Langerhans cells and Langerhans cell histiocytosis.

Silvia Lonardi*[1], Sara Scutera*[2], Sara Licini[1], Luisa Lorenzi[1], Anna Maria Cesinaro[3], Luisa Benerini Gatta[1], Carlotta Castagnoli[4], Daniele Bollero[5], Rosaria Sparti[2], Michela Tomaselli[1], Daniela Medicina[1], Federica Calzetti[6], Marco Antonio Cassatella[6], Fabio Facchetti[1], Tiziana Musso[2], William Vermi[1,5]

*equally contributed to this work

[1]Department of Molecular and Translational Medicine, University of Brescia, Brescia, Italy
[2]Department of Public Health and Pediatric Sciences, University of Turin, Turin, Italy
[3]Department of Anatomic Pathology, Modena University Hospital, Modena, Italy.
[4]Skin Bank, Department of General and Specialized Surgery, A.O.U. Città della Salute e della Scienza, Turin, Italy.
[5]Department of Surgery, Division of Plastic and Reconstructive Surgery and Burn Center, AOU Città della Salute, CTO Hospital, Turin, Italy.
[6]Section of General Pathology, Department of Medicine, University of Verona, Verona, Italy
[7]Department of Pathology and Immunology, Washington University, Saint Louis, Missouri.

Short title: CSF1R in Langerhans cells and LCH.

Keywords: Langerhans cells, LCH, CSF1R, Langerhans cells histiocytoses, BRAF

*To whom correspondence should be addressed:

William Vermi, MD, PhD

email: william.vermi@unibs.it

Dept. of Molecular and Translational Medicine

Section of Pathology

P.le Spedali Civili 1, 25123 Brescia, Italy

tel ++39-030399-8425; Fax: -5377

Text word count: 5213
Abstract word count: 245
Number of Figures: 6
Number of Table: 1
Number of References: 58

Abstract

Langerhans cell histiocytosis (LCH) is a rare disorder characterized by tissue accumulation of CD1a^{+} CD207^{+} LCH cells. In LCH, somatic mutations of the *BRAF*^{V600E} gene have been detected in tissue LCH cells, bone marrow CD34^{+} hematopoietic stem cells, circulating CD14^{+} monocytes, and BDCA1^{+} myeloid DCs. Targeting *BRAF*^{V600E} in clonal LCs and their precursors is a potential treatment option for patients whose tumors have the mutation. The development of mouse macrophages and LCs is regulated by the CSF-1 receptor (CSF1R). In patients with diffuse-type tenosynovial giant cell tumors, CSF1R inhibition depletes tumor-associated macrophages (TAMs) with therapeutic efficacy; however, CSF1R signaling in LCs and LCH has not been investigated. We found through immunohistochemistry and flow cytometry that CSF1R is normally expressed on human CD1a^{+}CD207^{+} LCs in the epidermis and stratified epithelia. LCs that were differentiated from CD14^{+} monocytes, BDCA1^{+} DCs, and CD34^{+} cord blood progenitors expressed CSF1R that was downregulated upon maturation. Immature LCs migrated toward CSF1, but not IL34. Administration of the c-FMS/CSF1R kinase inhibitors GW2580 and BLZ945 significantly reduced human LC migration. In LCH clinical samples, LCH cells (including *BRAF*^{V600E} cells) and TAMs retained high expression of CSF1R. We also detected presence of transcripts for its ligand, CSF1, but not IL34, in all tested LCH cases. CSF1R and CSF-1 expression in LCH, and their role in LC migration and differentiation, suggests CSF1R signaling blockade as a candidate rational approach for treatment of LCH, including the *BRAF*^{V600E} and wild-type forms of the disease.

INTRODUCTION

Langerhans cell histiocytosis (LCH) is characterized by tissue accumulation of transformed cells with features of Langerhans cells (LC) (1). LCH occurs in children and adults, and ranges from a single site lesion to systemic forms (2). The diagnosis is based on radiological presentation combined with tissue infiltration of LCs identified by CD1a, CD207, and S100 protein. MAPK activation is recurrent in LCH due to somatic mutations of components of the pathway (3). The identification of *BRAF*^{V600E} with a mutation-specific antibody allows the confirmation of the clonal identity of most tissue-infiltrating LCs in LCH (4). *BRAF*^{V600E} is also detected in CD34^{+} hematopoietic progenitors, circulating CD11c^{+}CD14^{+} precursors (5,6), BDCA1^{+} myeloid DCs, and CD16^{+} non-classical monocytes, suggesting the presence of *BRAF*-mutated LCH cases within the group of myeloid neoplasia (5,6).

This new paradigm shift in the LCH pathogenesis predicts that clonal circulating precursors are driven to terminal LCs differentiation by the tissue cytokine milieu. In this context, CSF1R signaling *via* its cognate ligands CSF-1 and IL34 plays a relevant role in various biological processes leading to differentiation of monocyte-derived cells, particularly macrophages. Accordingly, CSF1R blockade has been proposed (7) as a therapeutic strategy in various cancers, with more than twenty recruiting clinical trials existing (https://clinicaltrials.gov/ct2/results?recrs=ab&cond=Cancer&term=csf1r&cntry=&state=&city=&dist=) that employ this strategy. Among available compounds, the RG7155/emactuzumab, a specific CSF1R humanized antibody, has been shown to deplete CSF1R-expressing tumor-associated macrophages in advanced cancer patients (7). In addition to macrophages, RG7155/emactuzumab depletes blood CD16^{+}, but not CD14^{+}, monocytes (7), which is consistent with their higher expression of surface CSF1R (7,8).

Although the role of CSF-1 in human DCs has been partially characterized (9,10), the effects of CSF1R blockade on DC subsets are poorly understood. In mice, LCs are tightly dependent on CSF1R signaling for their development and maintenance (9). Mouse CSF1R binds CSF-1 and IL34, the latter being able to promote LC differentiation and maintenance in adulthood (10,11). In humans, CSF1R is expressed on DC progenitors and monocyte-derived DCs (8,12,13), whereas circulating and tissue conventional myeloid DCs are negative for CSF1R expression (8,14) and are not dependent on CSF1R for their development (15). High serum concentration of CSF-1 has been detected in LCH, particularly in the systemic forms (16,17). In addition, activating mutations in CSF1R have been identified in histiocytic neoplasm (18). However, CSF1R expression and

signaling involvement in human LCs and LCH has not been addressed.

In this study, we found that CSF1R was expressed in immature human CD207^{+} LCs, whereas it was lost upon LC maturation, as well as in nodal interdigitating DCs. CSF1R engaged by CSF1, but not IL34, provided a effective chemotactic signal to LCs. In addition, CSF1R blockade impaired LC differentiation from hematopoietic precursors. LCH cells and tumor-associated macrophages retained CSF1R, as verified in clinical samples. Together, these findings suggest CSF1R blockade as a candidate for the treatment of LCH.

METHODS

Tissue and immunohistochemistry

Formalin-fixed paraffin-embedded (FFPE) tissue blocks from normal skin (n=5), lung (n=2), esophagus (n=2), cervix (n=2), tonsils (n=2), reactive lymph nodes (n=2), dermatopatic lymphadenitis (n=12), as well as pathological tissues including Langerhans cell histiocytosis (n=54), cutaneous squamous cells carcinoma (n=5), primary cutaneous melanoma (n=9), and mycosis fungoides (n=3) were used. Cases were retrieved from the tissue archive of the Department of Pathology, ASST Spedali Civili di Brescia (Italy) and from Azienda Ospedaliero Universitaria, Modena (Italy). LCH cases inclusion criteria were expression of CD207 and CD1a in the majority of neoplastic cells. The study has been conducted according to the Declaration of Helsinki and approved by the local ethic board (NP906- WV-IMMUNOCANCERhum). Four-micrometer-thick tissue sections were used for immunohistochemical staining. Immunohistochemistry was performed after appropriate antigen retrieval (40' in thermostatic waterbath in EDTA buffer pH8.0 for CSF1R and BDCA1) using antibodies reported in **Supplementary Table S1**. Single immune reactions were developed using Novolink™ Polymer Detection System (cat. no. RE7280-K, Leica Biosystems, NewCastle upon Tyne, UK). For double/triple immunohistochemistry, the second immune reaction was visualized using Mach 4 Universal AP-Polymer Kit (cat. no. M4U536L, Biocare Medical, Concord, CA) followed by Ferangi Blue (cat. no. FB813S, Biocare Medical); sequentially the third immune reaction was visualized using Dako REAL™ Detection System, Alkaline Phosphatase/RED (cat. no. K5005, Dako, Glostrup, Denmark). BRAF (VE1) was stained by BenchMark ULTRA IHC/ISH system (cat. no 05342716001, Roche Diagnostics).

LCs purification from human skin.

Primary LCs and dermal DCs were purified from normal human skin (n=10) obtained as discarded material from reduction abdominoplasty after written consent, according to a protocol approved by the CTO/Città della Salute e della Scienza Hospital Ethical Board (Torino, Italy) and in adherence with the Declaration of Helsinki Principles. Following excision of subcutaneous fat, skin was cut in strips and exposed to dispase. Briefly, the skin was digested with 1U/ml dispase (cat. no. 17105041, Thermo Fisher Scientific, Waltham, MA), and penicillin-streptomycin solution overnight at 37°C, and the epidermis was peeled off the dermis. Dermal and epidermal sheets were then incubated separately in media containing 1% FBS (cat. no. 10270-106, Thermo Fisher Scientific), 200U/ml collagenase (cat. no. C5138) and 100U/ml DNase I (cat. no. 10104159001) (Sigma-Aldrich, Milan, Italy) at 37°C in a rotator for 30 min and 2 h, respectively. The cells were then separated using a tea

strainer (700 μm mesh size) and the supernatants were then passed through a 100 μm cell strainer for two times. For epidermal suspension, cells were spun at 400 g for 30 min on a Ficoll-Paque PLUS (cat. no. GE17-1440-02, GE Healthcare Bio- Sciences, Sigma-Aldrich) gradient and the immune cells harvested. Dermal cells were enriched for

CD45 expressing cells using magnetic beads (cat. no.130-045-801, Miltenyi, Bergisch Gladbach, Germany). Cells were then counted and labeled for flow cytometric evaluation of surface expression markers. In some experiments, cells enriched for CD45 (containing LCs) from the epidermis were left untreated or stimulated for 48 h with LPS (1 ug/ml) and R848 (5 ug/ml).

LC generation

Buffy coats were obtained from healthy blood donors (CPVE-S.Anna, Turin). Peripheral blood mononuclear cells enriched by Ficoll and $CD14^+$ monocytes and $BDCA1^+$ DCs isolated using anti-CD14–coated beads and human $BDCA1^+$ DC Isolation Kit (cat. no. 130-090-506, Miltenyi). To obtain LC-like DCs, $CD14^+$ monocytes were cultured for 7 days into in RPMI 1640 (cat.no. 21875034, Thermo Fisher Scientific) with 10% FCS (cat. no. 10270-106, Thermo Fisher Scientific) supplemented with GM-CSF (200 ng/ml, cat.no. 300-03), IL4 (20 ng/ml, cat. no. 200-04), and TGFβ (10 ng/ml, cat. no. 100-21C) (all from PeproTech, London, UK) (referred to as monocyte-derived LCs; mo-LCs). $BDCA1^+$ DCs were differentiated for 3 days with GM-CSF (100 ng/ml) and TGFβ (10 ng/ml) (referred as $BDCA1^+$ LCs). When required, LC-like DCs were matured with LPS (100 ng/ml, cat.no. L4391, Sigma-Aldrich) and R848 (1 μg/ml, cat. no. tlrl-r848, InvivoGen, Toulouse, France). Cord blood was obtained from Banca del Sangue Placentare following informed consent. $CD34^+$ progenitors were purified from cord blood with CD34 magnetic beads (cat. no. 130-100-453, Miltenyi) and cultured to induce LC-like cells (referred as $CD34^+$-LCs) in X-VIVO 15 media (cat. no.04-448Q, Lonza, Walkersville, MD) with GM-CSF (100 ng/ml), SCF (20 ng/ml, cat. no. 300- 07), Flt3 (100 ng/ml, cat. no. 300-19), TNFα (2.5 ng/ml, cat. no. 300-01A), and TGFβ1 (5 ng/ml) (all from PeproTech) for 10 days. In differentiation experiments cells were cultured with CSF-1 (100 ng/ml, cat. no. 300-25) or GM-CSF in combination with the other cytokines for respectively 14 and 10 days. In some experiments, $CD34^+$ cells were cultured with GM-CSF or CSF-1 in combination with the other cytokines for 12 and 22 days. Cells were differentiated in absence or presence of BLZ945 (0.5 μM, cat. no. S7725Selleckchem, Munich, Germany) added after 7 days.

Flow cytometry

In vitro differentiated LCs were stained using antibodies detailed in **Supplementary Table S1** and analyzed using BD FACSCalibur (BD Biosciences, San Josè, CA). For dermal and epidermal DCs, cells were stained with antibodies indicated in **Supplementary Table S1**. Viability was assessed with Viability 405/520 Fixable Dye (cat. no. 130-109-814, Miltenyi) diluted 1:100 or with LIVE/DEAD™ Violet Viability dye (cat. no. L34955, Thermo Fisher Scientific) diluted 1:1000. To minimize FcR-mediated mAb binding, cells were stained in the presence of human serum

containing IgG (cat. no. I2511, Sigma-Aldrich) and Tandem Signal Enhancer (cat. no. 130-099-888, Miltenyi) to reduce non-specific binding of tandem dye–conjugated antibodies to human cells. Briefly cells ($1x10^6$) were washed in buffer containing PBS pH 7.2, 0.5% bovine serum albumin (BSA), and 2 mM EDTA and stained for viability and blocking before specific antibody staining (incubated for 15 minutes in the dark in the refrigerator). Cells were then washed and fixed in 1% paraformaldehyde and acquired using MACSQuant (Miltenyi) or BD FACSVerseTM (BD Biosciences). Analysis was performed with FlowLogic software.

Cell sorting for preparation of cell blocks

Fresh PBMCs were isolated from buffy of healthy donor coat by density centrifugation using Ficoll-Paque gradient (GE Healthcare). For purification of monocytes populations and $BDCA1^+$ dendritic cells PBMCs were stained with the following panel of human antibodies: FITC-CD14 (clone TUK4, cat.no. 130-113-146, Miltenyi), PE-CD56 (clone AF12-7H3, cat.no. 130-090-755, Miltenyi), perCP-Cy5.5–CD16 (clone 3G8, cat. no. 302030 Biolegend, San Diego, CA), PE-VIO770–CD3 (clone REA613, cat. no. 130-113-140, Miltenyi), PE-VIO770 CD20 (clone LT20, cat. no. 130-113-375, Miltenyi), APC-CD303 (clone AC144, cat. no. 130-090-905, Miltenyi), APC-CD141 (clone AD5-14H12, cat. no. 130-113-314, Miltenyi) and APC-Cy7–HLA-DR (clone L243, cat. no. 307618, Biolegend) and sorted using FACSAria II (BD Biosciences). Accordingly, PBMCs were subjected to doublets exclusion and subsequently gated on lymphocytes negative (CD3, CD19 and CD56) and HLA-DR positive cells, finally monocytes were positively selected as $CD14^+CD16^-$ or $CD14^-CD16^+$ whereas $BDCA1^+$ were negatively selected as $CD14^-CD16^-CD141^-$ and $CD303^-$. Fluorescence negative controls were performed using intra-simple negative populations as reference.

For cell block preparation, cell suspensions of sorted cells were centrifuged for 10 minutes at 3,000 rpm. A solution of plasma (100 mL, kindly provided by Centro Trasfusionale, ASST Spedali Civili) and HemosIL RecombiPlasTin 2G (200 mL, Instrumentation Laboratory; cat. no. 0020003050; 1:2) were added to cell pellets, mixed until the formation of a clot, then placed into a bio-cassette (Bio-Optica; cat. no. 07-7350). The specimen was fixed in 10% formalin (Bio-Optica; cat. no. 05-K01004) for 1 hour followed by paraffin inclusion.

LC migration assay

Migration of mo-LCs was measured in triplicate with a transwell system (cat. no.3421, 24-well plates; 5.0 µm pore size; Corning Costar, NY). RPMI 1640 with 1% FCS alone, with varying doses

of M-CSF or IL34 (cat. no. 200-34, PeproTech) added to the lower chamber. Wells with medium alone were used as a control for spontaneous migration. A total of 2.5×10^5 cells in 200 µl was added to the upper chamber and incubated at 37°C for 4 h. In some migration experiments, cells were pretreated with GW2580 (1uM, cat. no. SML1047, Sigma-Aldrich) or with BLZ945 (0.5 µM, Selleckchem) for 60 min at 37°C. For migration of BDCA1$^+$ LC, 1.5×10^5 cells in 200 µl were added to the upper chamber of a transwell system (5.0 µm pore size; Corning Costar) and harvested after 6 h of migration towards M-CSF (50 ng/ml). Mo-LCs and BDCA1$^+$ LCs were not enriched for CD207. Cells migrated into the lower chamber were harvested, concentrated to a volume of 300 µl of PBS, and counted by flow cytometry. Events were acquired for a fixed time of 60 s. The counts fell within a linear range of the control titration curves obtained by testing increasing cell concentrations. Values are given as the mean number of migrated cells ± SEM.

Apoptosis assay

Mo-LC were incubated in RPMI 10% FCS for 48 h in presence or absence of M-CSF or IL34 (50 ng/ml), to evaluate their capacity of protection. Cells were washed, resuspended in Annexin Buffer, and evaluated for apoptosis using the annexin V-FITC apoptosis detection kit (cat. no.640914, Biolegend).

***BRAF* genotyping by digital PCR**

DNA of twenty LCH cases (details in **Supplementary Table S2**) was extracted from sections of archival paraffin blocks using the QIAamp DNA FFPE Tissue Kit (cat. no. 56404, QIAGEN, Venlo, Netherlands). QX200 Droplet Digital PCR system (Bio-Rad, Hercules, CA) was used for analysis of *BRAF*^{V600E} mutation. ddPCR reagents were purchased from Bio-Rad and included the ddPCR Mutation Assay *BRAF* V600E FAM/HEX. *BRAF*^{V600E} cutaneous melanomas were included as positive control sample. The droplet emulsions were thermally cycled with the use of the following protocol: denaturation at 95°C for 10 minutes, followed by 40 cycles of 94°C for 30 seconds and 55°C for 1 minute. After cycling, a final 10-minute hold at 98°C was applied to deactivate the enzyme and to stabilize the droplets. Experiments have been performed in duplicate.

Gene expression profile by digital droplet PCR (ddPCR)

Expression profile for selected targets was performed by ddPCR using the Bio-Rad QX200 ddPCR platform. Briefly, RNA of twelve LCH cases from skin, lung, bone and lymph node (#6, #13, #16, #19, #31, #35, #40, #44, #45, #47, #50, #51; see **Supplementary Table S2** for details) was extracted from sections using RNeasy FFPE Kit (cat. no. 73504, QIAGEN). The cDNAs were

synthesized from total RNA using iScript gDNA Clear cDNA Synthesis Kit (cat. no. 1725035, Bio-Rad), in a volume of 20 µl, prior to droplet formation. The RNA expression for all targets was normalized to UBC expression. The human PrimePCR™ ddPCR™ Expression Probe Assays (Bio-Rad) were used at a final concentration of 1X and include KRT14 dHsaCPE5192231, CSF1R dHsaCPE5042034, CSF-1 dHsaCPE5042260, IL-34 dHsaCPE5038840, CD207 dHsaCPE5035151 and UBC dHsaCPE5190156. All assays were analyzed using QuantaSoft Software (Bio-Rad).

Statistical Analysis

Statistical significance was determined by using non-parametric Student *t* test or ANOVA followed by Tukey's Multiple Comparison Test, as appropriate. Results were analyzed by using GraphPad PRISM5.0 software.

RESULTS

CSF1R expression in human intraepithelial LCs and tumor-associated LCs

We tested CSF1R expression on human tissues by using a CSF1R antibody (clone FER216) that recognizes CSF1R on CD16$^+$ and CD14$^+$ circulating monocytes (7,8) from cell block preparations (**Supplementary Fig. S1A**), CD68$^+$ macrophages in reactive lymph nodes, and TAMs in human lymphomas, but that results negative on most lymphoid cells (19). In normal skin (n=2), tonsil (n=2), lung (n=2), esophagus (n=2), and uterine cervix (n=2), most of the CD1a$^+$CD207$^+$ LCs within the epithelium express CSF1R (**Fig. 1A-C, Supplementary Fig. S1B-D**). Moreover, macrophages in all of these tissues reacted to anti-CSF1R, as confirmed by coexpression of CD163 (**Fig. 1D**), whereas no reactivity could be detected by using an isotype control (**Supplementary Fig. S1E)**.

Dermal DCs in non-inflamed normal skin are typically sparse. We could expand the analysis in FFPE samples containing a sizeable number of dermal immune cells by measuring cDC1s (CD141$^+$), cDC2s (BDCA1/CD1c$^+$), and the previously identified dermal CD207$^+$ DC subset (12). We validated a BDCA1 antibody for FFPE using cell-block preparations of peripheral blood BDCA1$^+$ DCs (**Supplementary Fig. S1F)**. By using a set of markers including CD1a, BDCA1, CD207, and IRF4, we found that most dermal myeloid DCs were negative for CSF1R (**Fig. 1E-G**). This combination of antibodies confirmed the non-LC identity of the small fraction of CD207$^+$ dermal cells, as suggested by others (12). CD207$^+$ dermal DCs reacted to BDCA1 (**Fig. 1H**) and expressed IRF4, a cDC2 transcription factor **(Fig. 1I**) that is typically negative on LCs **(Fig. 1I upper right**). Our findings confirm a distinct cDC2 phenotype of CD207$^+$ dermal DCs in human tissue. Consistent with the immunohistochemistry results, flow cytometry analysis of human epidermal cell suspensions revealed CSF1R expression on LCs, the latter populations defined as CD1a$^+$CD207$^+$ cells within the CD45$^+$HLA-DR^{++} fraction (**Fig. 2A and Supplementary Fig. S2A**). As compared to freshly isolated LCs (**Fig. 2A**), a decrease in CSF1R expression on CD1a$^+$CD207$^+$ cells was observed after a 48h in epidermal CD45 enriched cell culture in the absence (14% reduction respect to freshly isolated cells) or, even more so, in the presence of stimulation with LPS and R848 (12% reduction respect to unstimulated cells) (**Fig. 2B**), indicating that CSF1R is downregulated during LC maturation. Analysis on dermal cell suspensions revealed a low expression of CSF1R on the CD1a$^+$CD207$^-$ (about 6%) and on the CD1a$^+$CD207$^+$ (about 2%) dendritic cells; in contrast, a higher percentage of CSF1R$^+$ cells was observed in the CD1a$^-$ fraction, likely corresponding to monocytes and dermal macrophages (**Supplementary Fig. S2B**).

CD207$^+$ tumor-associated LCs have been reported in various cutaneous cancers (20). We further expanded our analysis on cutaneous tumor-associated CD207$^+$ cells. We analyzed cutaneous melanomas (n=9), squamous cell carcinomas (n=5) and mycoses fungoides (n=3), and found that CD207$^+$CSF1R$^+$ cells were mainly confined to the intraepithelial compartment, whereas dermal CD207$^+$ cells largely lacked expression of CSF1R (**Supplementary Fig. S3**) and coexpressed the cDC2 markers IRF4 and BDCA1 **(Supplementary Fig. S3B, C, E, F)**.
Altogether, these findings establish that CSF1R is expressed in intraepithelial CD207$^+$ LCs but not in CD207$^+$ cDC2. This profile is similar in skin cancers.

CSF1R modulation during LC differentiation and maturation

LCs can be differentiated from monocytes or CD34$^+$ progenitor cells. In addition, circulating BDCA1$^+$ DCs are identified as an alternative source of LC precursors (12,21). LCH cells are presumed to arise from clonal BDCA1$^+$ DC precursors (22). We thus evaluated CSF1R expression on LCs obtained from different precursors. Surface CSF1R expression was found on about 60% of mo-LCs (n=6), as well as on LCs obtained from CD34$^+$ (n=4) and BDCA1$^+$ DC precursors (n=5) (**Fig. 3A**). In line with our observation on freshly-purified primary LCs (**Fig. 2B**), CSF1R expression was significantly downregulated in mature mo-LCs, in parallel with an upregulation of CD83 and IRF4 expression (**Fig. 3B**).
Nodal LC-like cells are undetectable in unstimulated lymph nodes, but they are easily identifiable within the lymphatic sinuses and in expanded T-cell nodules of the paracortex in the so-called dermatopathic lymphadenitis. This is a condition in which, following proinflammatory stimuli, LCs migrate to draining lymph nodes and undergo maturation. In the paracortex of human lymph nodes, the LC-like population has been referred by pathologists to as interdigitating dendritic cells (IDCs) and displays the S100$^+$CD1a$^+$CD207$^{+/-}$ phenotype. Expectedly, IDCs also coexpress a set of maturation markers such as CD80, CD83, CD208, and CCR7. By evaluating CSF1R expression on ten cases of dermatopathic lymphadenitis, we found CSF1R expression on macrophages in various nodal compartments (**Supplementary Fig. S4A)**, in line with published data (19). On the contrary, IDCs of the paracortex largely lacked CSF1R expression **(Fig. 3C, D)**, although it was possible to identify a small population of CSF1R$^+$CD207$^+$ within the nodal lymphatic sinuses (**Fig. 3D-F, Supplementary Fig. S4B-E**).
The notion that IDCs in the paracortex are mainly LC-derived has been challenged, particularly in the mouse system. Cells of non-LC identity and likely corresponding to cDC2s have been identified in the T cell paracortex (23). By analysis of dermatopathic lymphadenitis (n=4), CSF1R$^+$CD207$^+$ LCs within the nodal lymphatic sinuses lacked expression of BDCA1 and IRF4

(Fig. 3F and Supplementary Fig. S4B, C) and lacked the maturation markers CD83 and CD208 **(Supplementary Fig. S4D, E)**. On the contrary, most IDCs in the paracortical T-cell nodules expressed the transcription factor IRF4 (**Fig. 3G, H**). Further, we could identify two main IDC subpopulations showing a distinct localization (**Fig. 3H and Supplementary Fig. S4F, G**). Cells in the outer paracortex that coexpressed BDCA1 and IRF4, and expressed CD83 and CD208, likely correspond to mature cDC2 (**Fig. 3H**, **Supplementary Fig. S4G and H**). Nodal cDC2s can derive from circulating cDC2s *via* high endothelial venules or from migrating dermal cDC2s, including the CD207$^+$ minor subset. The second subpopulation was mainly located in the inner paracortex and included CD207$^+$BDCA1$^-$IRF4$^+$ cells (**Fig. 3H and Supplementary Fig. S4F, G**) coexpressing CD208 (**Supplementary Fig. S4G)**, likely corresponding to mature LCs; accordingly, we could demonstrate IRF4 induction upon *in vitro* maturation of LC (**Fig. 3B**). Of note, mouse dermal DCs migrate in the outer paracortex, whereas epidermal LCs are mainly found in the inner paracortical area (24). With some heterogeneity from case to case, we uncovered a third minor fraction of the BDCA1$^+$ in the paracortex coexpressing CD207 (**Supplementary Fig. S4G black arrow)**; a similar population was also found within the nodal sinuses, likely representing migrating dermal CD207$^+$ cDC2s (**Supplementary Fig. S4I**). Altogether, these findings suggest that CSF1R expression is tightly associated to LC differentiation but is lost upon maturation. Immature CSF1R$^+$LCs are confined to the nodal sinuses, whereas their maturation is coupled with loss of CSF1R. Moreover, a dermal cDC2 identity of a fraction of CSF1R$^-$ IDCs should be considered.

CSF1R inhibition impairs LC migration and differentiation.

CSF1R signaling is relevant during macrophage proliferation and differentiation (25). CSF1R blockade in tumor-bearing mice and cancer patients results in depletion and molecular reprogramming of tumor associated-macrophages (26). CSF1R-induced cell migration plays an important role in macrophage trafficking to tumor tissues (27). We examined the ability of mo-LCs to migrate towards CSF-1 and IL34 (n=4). CSF-1 showed a significant chemotactic effect at 50 ng/ml that is maintained at 200 ng/ml (**Fig. 4A,** left panel and **Supplementary Fig. S5A**). No effect of IL34 on mo-LCs migration was observed (**Fig. 4A,** left panel and **Supplementary Fig. S5A**). The migration toward CSF-1 diminished following treatment with the c-FMS/CSF1R kinase inhibitors GW2580 and BLZ945 (**Fig. 4A**, middle panel). The chemotactic effect of CSF-1 was also demonstrated in BDCA1$^+$ DC-derived LCs (**Fig. 4A**, right panel). Since IL34 and CSF-1 have been shown to promote cell survival (28), we investigated the role of these two cytokines in mo-LC viability (n=4). No significant differences were observed in the percentage of live mo-LCs following IL34 and CSF-1 treatment compared to untreated cells (**Supplementary Fig. S5B**). Data

on the role of CSF-1 on the differentiation of $CD207^+$ cells from precursors are largely missing in the literature. We generated LCs from $CD34^+$ progenitor (n=3) cells in presence of the standard cytokine cocktail (SCF, Flt3L, TNFα, and TGFβ1) in combination with CSF-1 and compared to GM-CSF (**Fig. 4B)**. CSF-1 induced a consistent differentiation in $CD1a^+CD207^+$ cells (88.3±2.7%) and the blockade of the CSF1/CSF1R signaling with BLZ945 significantly reduced differentiation (53±6.7%) of $CD1a^+CD207^+$ cells (p = 0.0083). The percentage of $CD1a^+CD207^+$ cells recovered from CSF-1 culture was higher than that obtained from GM-CSF culture, and the latter was not affected by BLZ945 (**Fig. 4B**, right panel; p= 0.83). Based on the different kinetics of differentiation between the two experimental conditions (29) (30), the analysis was performed at 10 and 14 days of culture, respectively for GM-CSF and CSF1. However, the BLZ945 effect on CSF-1 but not GM-CSF culture was also confirmed when cells were treated for the same length of time (12 and 22 days) (**Supplementary Fig. S6**). The cell recovery yield was higher for GM-CSF culture compared with CSF1. Specifically, starting from $0.2x10^6$ $CD34^+$ cells the absolute number of viable cells recovered from GM-CSF culture was $11.2 \pm 4.8 \times 10^6$ (56 ± 24 fold increase), but no differences were observed after BLZ945 treatment (p= 0.975). The yield of cells from CSF-1 culture was $3.3 \pm 0.8 \times 10^6$ (17 ± 3.9 fold increase) but was significantly reduced by the addition of BLZ945 (p= 0.039).

These results indicate that CSF-1 regulates LC migration and may induce LC differentiation from $CD34^+$ precursors.

CSF1R expression in neoplastic cells and TAMs in Langerhans cells histiocytosis.

Clonally transformed LCs are found in LCH (1). LCH biopsies show tissue infiltration of $CD1a^+CD207^+S100^+$ LCs on a background of inflammatory cells including eosinophils and macrophages. We tested the expression of CSF1R in a large retrospective cohort of LCH biopsies (n=54) including 9 multisystemic disease (**Table 1 and details in Supplementary Table S2**). Two representative cases are illustrated in **Figure 5**. LCH diagnosis was defined based on the morphology and phenotype of LCH cells using CD1a, CD207, and S100 (**Fig. 5A-T)**. In addition, LCH cases were tested for *BRAF*^{V600E} mutation by immunohistochemistry **(Fig. 5E, J, O, T; Supplementary Table S2 and Supplementary Fig. S7**) and droplet digital PCR **(Supplementary Table S2 and Supplementary Fig. S7E, J, O**). We found that CSF1R was expressed in all cases **(Supplementary Table S2)**. The stain was observed in the cytoplasm as well as on the cell membrane (n= 33/54; 61,1% of LCH cases) (**Fig. 5I, Supplementary Fig. S7C, H, M and Supplementary Table S2**). CSF1R expression on tissue LCH cells was confirmed in serial sections (**Supplementary Fig. S7**) and by its colocalization with cytoplasmic anti-VE1, recognizing the

BRAF^{V600E} mutant (**Fig. 5U-W**). We could confirm CSF1R reactivity also by using a second antibody (clone SP211, rabbit monoclonal) recognizing a portion of the intracellular domain of CSF1R **(Supplementary Fig. S8)**. In addition to neoplastic cells, anti-CSF1R also reacted with surrounding CD163^{+} tumor-associated macrophages (**Fig. 5X**).

Based on the down-modulation of CSF1R in matured LCs, we tested the phenotype of neoplastic LCs in a set of LCH cases (n=9). Most neoplastic LCH cells regularly display an immature phenotype, as previously reported (31), largely lacking expression for CD83, CD208, and CCR7 (**Supplementary Fig. S7P–R**). Findings suggest that circulating LCH cells display a cDC2 phenotype and likely represent immediate precursors of transformed LC cells (22). Staining for BDCA1 and CD207 confirm a highly frequent (n= 43/43; 100%) and diffuse expression of BDCA1 on tissue CD207^{+} LCH cells (**Supplementary Fig. S7S–T**). Coexpression of IRF4 with CD207 was frequently observed (n= 35/46; 76,1%), although it was highly heterogeneous in its distribution (**Fig. 5Y and Supplementary Table S2**). This hybrid phenotype indicates that, in more than two thirds of the cases, tissue LCH cells are cDC2-derived. However, CSF1R expression in LCH is stably retained irrespectively of their phenotype. In addition, CSF1R expression is also found in surrounding TAMs, indicating that both cell types might be targeted by CSF1R blockade.

CSF-1 transcript and phospho-p44/42 expression in LCH tissues.

We next analyzed the expression of CSF1, CSF1R, and IL34 in a group of twelve LCH cases, with available archival material including skin and extra-cutaneous LCH, by digital droplet PCR. Keratin 14 (KRT14) and CD207 were used as markers of epidermal keratinocytes and neoplastic LCH-cells. Accordingly, KRT14 transcript expression was limited to skin biopsies, whereas CD207 expression was often found to be comparable in skin and extra-cutaneous LCH. We could detect expression of CSF-1 (10/12; 83.3%) and CSF1R (12/12; 100%) in the large majority of the LCH cases (**Fig. 6A, B**), whereas IL34 expression was largely absent. CSF1R engagement by CSF-1 results in downstream activation of the MAPK pathway. Similar to *BRAF*-mutated cases (n=8) (**Supplementary Fig. S9**), in *BRAF* wild-type cases (n=6), CSF1R^{+} neoplastic cells frequently stained for anti–phospho-p44/42 MAPK (Thr202/Tyr204) as demonstrated in serial sections; anti–phospho-p44/42 was also detected in some tumor-associated macrophages (**Fig. 6C-H**). These findings suggest MAPK pathway activation also occurs in the absence of *BRAF* mutations and might partially rely on CSF1R signaling.

DISCUSSION

LCs are specialized dendritic cells located within the epithelial surface. During inflammation, LCs can arise from CD34$^+$ progenitors, classical monocytes, and BDCA1$^+$ blood cDC2s (9,32). Data suggest that murine LC development is dependent on CSF1R signaling (10,11,33), but limited data are available on its expression and function in human LCs. We report here that CSF1R was expressed by human LCs and was involved in LC migration towards CSF1. CSF1R stained LCH cells and TAMs, whereas CSF-1 was abundantly produced in neoplastic tissues. CSF1R was expressed in normal LCs, tumor-associated LCs infiltrating skin cancer, and in nodal LCs within the lymphatic sinuses of dermatopathic lymphadenitis. On the contrary, most dermal myeloid DCs, including a minor subset of CD207$^+$, lacked CSF1R. We demonstrated surface CSF1R on LCs isolated from human skin and on immature LCs *in vitro* generated from CD34$^+$ progenitors, CD14$^+$ monocytes, and BDCA1$^+$ cells, by using published protocols (32,34).

The role of tumor-associated LCs has been partially investigated in skin cancer (35). Based on our study, CSF1-producing tumors might modulate the LC contexture at different sites, particularly in lymph nodes draining skin cancer. Similar to TAMs (7,36), LCs might represent a relevant cell target during therapeutic CSF1R blockade. This hypothesis is further strengthened by our observation that CSF1R signaling was involved in LC expansion from CD34$^+$ precursors, suggesting that CSF1R blockade could result in a more dramatic and stable defect of the LC pool in these patients. We found that the presence of CSF-1 during CD34$^+$ differentiation gave rise to a higher fraction of CD1a$^+$CD207$^+$ LCs that was reduced by CSF1R blockade. Our study corroborates previous observations (29,37) on the role of CSF-1 on the LC differentiation. We have not monitored LC precursors at various stage of differentiation during CSF-1 culture and CSF1R blockade. However, it is known that CD1a$^-$CD14$^+$CSF1R$^+$ LC precursors require exogenous TGFβ (38). In addition, monocyte and DC progenitor cells express CSF1R (13). The effect of CSF-1 and CSF1R-blockage in LCs will certainly benefit from additional preclinical modelling and clinical monitoring on cancer patients.

After receiving local signal, LCs migrate to draining lymph nodes. A set of proinflammatory stimuli and chemokines are required for LC migration to the nodal paracortex in form of LC-derived S100$^+$CD1a$^+$CD207$^{+/-}$ IDCs. We found that CSF1R is expressed by immature LCs confined to the nodal sinuses, but it is rapidly downregulated upon maturation; in line with this observation, downregulation of CSF1R was documented in DCs exposed to TNF (39). In contrast with LCs, most IDCs lacked expression of CSF1R. Lack of CSF1R on IDCs could be a function of their mature phenotype, as demonstrated in this study. Alternatively, a non-LC identity has been

proposed for IDCs (23), and other studies have demonstrated a cDC2 phenotype of IDCs (23). We found that a fraction of IDCs, particularly those located in the outer paracortex, mainly display a mature cDC2 phenotype, whereas IDCs in the inner paracortex more likely correspond to mature LCs.

In the current study, the expression of CSF1R in LCH biopsies was demonstrated by using two antibodies recognizing different CSF1R domains, and CSF1R reactivity was detected on LCH cells and TAMs. In *BRAF*–wild-type cases, CSF1R$^+$ cells coexpressed phospho-p44/42, suggesting CSF1R-dependent persistent activation of the MAPK pathway (28). Subcellular distribution of CSF1R in LCH cells included cytoplasmic and membrane localization. The observed subcellular heterogeneity may be consistent with the receptor compartmentalization during activation and subsequent degradation (40,41). Alternatively, genomic abnormalities at the CSF1R locus or post-transcriptional modification occurring in LCH cells, as observed in other cancers, might explain this variability (42).

IL34 was identified as an alternative ligand of CSF1R showing overlapping functions with CSF-1 with respect to myeloid lineage differentiation, proliferation, and survival (43). Of note, we found that CSF-1 was a potent chemoattractant for LCs, whereas IL34 showed no activity. These results support the notion that the two cytokines are partially redundant, as demonstrated by their different ability to induce morphological changes and cytokines production in macrophages (44). Previous data confirms the role of CSF1R signaling in the chemotaxis of mononuclear phagocytes (45). CSF-1 is highly expressed in carcinomas and sarcomas from different primary sites (46), whereas no data are available on LCH biopsies. We found that in contrast with IL34, CSF-1 is abundantly produced in cutaneous and extra-cutaneous LCH tissue. This finding might explain the high serum concentration of CSF-1 in patients with multisystemic LCH (16,17) and suggests that CSF1R$^+$ LCH cells are recruited to neoplastic tissues by high local amounts of CSF1, as also reported in diffuse-type Tenosynovial Giant Cell Tumor (47).

Reports on systemic LCH indicate a hematopoietic origin of LCH cells. Clonal circulating precursors can be detected in form of CD34$^+$ progenitors, monocytes and cDC2s (5,6), likely representing immediate precursors of LCH cells (22). High serum concentrations of TGFβ and CSF-1 have been found in LCH patients, suggesting their contribution in the differentiation of tissue-infiltrating neoplastic LCs from hematopoietic precursors (48). Transcriptomic studies revealed a monocyte-LC signature for LCH cells driven by JAG2-mediated activation of Notch

(49). We observed a hybrid phenotype of *BRAF*^{V600E} LCH cells, with cDC2 markers (BDCA1^{+} and IRF4^{+}) admixed to LC markers (CD1a, CD207, and CSF1R) indicating that a partial LC commitment of cDC2 circulating precursors might also occur. Since CSF1R is required for terminal LC differentiation from CD34 precursors, as shown in the current study, we propose that CSF1R blockade might improve the LCH evolution.

In conclusion, although we recognize that additional data on fresh LCH cells are required to confirm our findings, we propose that LCH cases (and likely other LC/macrophage derived neoplasms) might derive benefit from CSF1R blockade, a hypothesis suggested previously on preliminary findings (9). The relevance of this recommendation is further strengthened by the identification of activating CSF1R mutations in histiocytic neoplasm, with mutated tumor cells resulting sensitive to CSF1R blockade (18,50). We envisage a synergistic clinical benefit by targeting tissue LCH cells (and their circulating precursors) and TAMs. Of note, CSF1R expression is also detected in the *BRAF*^{V600E} mutated forms of LCH, a candidate group for BRAF inhibitors (51,52) as a treatment option (53). However, the clinical benefit of MAPK inhibition in these patients is transient with frequent relapse (54-56), suggesting that additional treatment options are required for life-threatening LCH. Responders to CSF1R blockade will be likely enriched in the *BRAF* wild-type subgroup. However, concomitant or sequential combination of BRAF- and CSF1R-blockade could be effective in *BRAF*^{V600E} LCH, as observed in preclinical models of melanomas (57,58), although it remains to be established how these compounds cooperate in LCH.

Acknowledgments

We greatly appreciate the help from Dr. Carola Ries by reading our manuscript and providing excellent comments. We are grateful to Fondazione Beretta (Brescia, Italy) for support to Silvia Lonardi, Michela Tomaselli and Sara Licini. We like to thank pathologists, technicians, clinicians, nurses and administrative employers that have provided support to the study and to the follow-up of LCH patients. We like to acknowledge AIRC for its financial support (IG 15378-2014 and IG 23179 to WV). We are grateful to Mattia Bugatti for his excellent support on preparation of human tissue biopsies.

Authors contributions

W.V supervised the study; W.V and T.M designed the study; W.V, T.M, S.Lon and S.S wrote the manuscript; W.V, T.M, S.Lon, S.S and M.A.C interpreted the results; S.Lon, S.S, S. Lic, L.B, D.M, F.C and M.T. performed the experiments; L.L, A.M.C, F.F provided LCH cases; C.C, D.B and R.S

provided and performed experiments on ex vivo dendritic cells skin sample; S. Lon, S.S, L.L, A.M.C, M.A.C, F.F, T.M, W.V revised the manuscript.

All authors have read, commented and approved the manuscript in its final form.

Disclosure of Potential Conflicts of Interest

All the authors declare no competing financial interests.

Table 1. Summary of LCH cases analyzed

Site of LCH lesion	**Number of cases**	**Median age (year range)**	**gender (M;F)**	***BRAF*** ^{V600E} **(%)**	**MD (%)**
Skin	16	15,4	11;5	8 (36,4)	6 (27,3)
Bone	20	17	13;7	8 (40)	0 (0)
Soft Tissue	5	15	1;4	2 (40)	1 (20)
Lung	5	28,8	1;4	4 (80)	0 (0)
Lymph node	4	41,6	2;2	0 (0)	1 (25)
Other localization	4	17,25	2;2	3 (75)	1 (25)
TOTAL	**54**	**22,5 (1 DAY-79 YEARS)**	**30;24**	**25 (41,7)**	**9 (15)**

Legend: MD= multisystemic disease

REFERENCES

1. Haroche J, Cohen-Aubart F, Rollins BJ, Donadieu J, Charlotte F, Idbaih A*, et al.* Histiocytoses: emerging neoplasia behind inflammation. The Lancet Oncology **2017**;18(2):e113-e25 doi 10.1016/S1470-2045(17)30031-1.
2. Haupt R, Minkov M, Astigarraga I, Schafer E, Nanduri V, Jubran R*, et al.* Langerhans cell histiocytosis (LCH): guidelines for diagnosis, clinical work-up, and treatment for patients till the age of 18 years. Pediatric blood & cancer **2013**;60(2):175-84 doi 10.1002/pbc.24367.
3. Diamond EL, Durham BH, Haroche J, Yao Z, Ma J, Parikh SA*, et al.* Diverse and Targetable Kinase Alterations Drive Histiocytic Neoplasms. Cancer discovery **2016**;6(2):154-65 doi 10.1158/2159-8290.CD-15-0913.
4. Sahm F, Capper D, Preusser M, Meyer J, Stenzinger A, Lasitschka F*, et al.* BRAFV600E mutant protein is expressed in cells of variable maturation in Langerhans cell histiocytosis. Blood **2012**;120(12):e28-34 doi 10.1182/blood-2012-06-429597.
5. Berres ML, Lim KP, Peters T, Price J, Takizawa H, Salmon H*, et al.* BRAF-V600E expression in precursor versus differentiated dendritic cells defines clinically distinct LCH risk groups. The Journal of experimental medicine **2015**;212(2):281 doi 10.1084/jem.2013097701202015c.
6. Durham BH, Roos-Weil D, Baillou C, Cohen-Aubart F, Yoshimi A, Miyara M*, et al.* Functional evidence for derivation of systemic histiocytic neoplasms from hematopoietic stem/progenitor cells. Blood **2017**;130(2):176-80 doi 10.1182/blood-2016-12-757377.
7. Ries CH, Cannarile MA, Hoves S, Benz J, Wartha K, Runza V*, et al.* Targeting tumor-associated macrophages with anti-CSF-1R antibody reveals a strategy for cancer therapy. Cancer cell **2014**;25(6):846-59 doi 10.1016/j.ccr.2014.05.016.
8. Micheletti A, Finotti G, Calzetti F, Lonardi S, Zoratti E, Bugatti M*, et al.* slan/M-DC8+ cells constitute a distinct subset of dendritic cells in human tonsils. Oncotarget **2016**;7(1):161-75 doi 10.18632/oncotarget.6660.
9. Ginhoux F, Tacke F, Angeli V, Bogunovic M, Loubeau M, Dai XM*, et al.* Langerhans cells arise from monocytes in vivo. Nature immunology **2006**;7(3):265-73 doi 10.1038/ni1307.
10. Wang Y, Szretter KJ, Vermi W, Gilfillan S, Rossini C, Cella M*, et al.* IL-34 is a tissue-restricted ligand of CSF1R required for the development of Langerhans cells and microglia. Nature immunology **2012**;13(8):753-60 doi 10.1038/ni.2360.
11. Greter M, Lelios I, Pelczar P, Hoeffel G, Price J, Leboeuf M*, et al.* Stroma-derived interleukin-34 controls the development and maintenance of langerhans cells and the maintenance of microglia. Immunity **2012**;37(6):1050-60 doi 10.1016/j.immuni.2012.11.001.
12. Bigley V, McGovern N, Milne P, Dickinson R, Pagan S, Cookson S*, et al.* Langerin-expressing dendritic cells in human tissues are related to CD1c+ dendritic cells and distinct from Langerhans cells and CD141high XCR1+ dendritic cells. Journal of leukocyte biology **2015**;97(4):627-34 doi 10.1189/jlb.1HI0714-351R.
13. Breton G, Lee J, Zhou YJ, Schreiber JJ, Keler T, Puhr S*, et al.* Circulating precursors of human CD1c+ and CD141+ dendritic cells. The Journal of experimental medicine **2015**;212(3):401-13 doi 10.1084/jem.20141441.
14. Calzetti F, Tamassia N, Micheletti A, Finotti G, Bianchetto-Aguilera F, Cassatella MA. Human dendritic cell subset 4 (DC4) correlates to a subset of CD14(dim/-)CD16(++)

monocytes. The Journal of allergy and clinical immunology **2018**;141(6):2276-9.e3 doi 10.1016/j.jaci.2017.12.988.

15. Kashem SW, Haniffa M, Kaplan DH. Antigen-Presenting Cells in the Skin. Annual review of immunology **2017**;35:469-99 doi 10.1146/annurev-immunol-051116-052215.
16. Rolland A, Guyon L, Gill M, Cai YH, Banchereau J, McClain K, *et al.* Increased blood myeloid dendritic cells and dendritic cell-poietins in Langerhans cell histiocytosis. Journal of immunology **2005**;174(5):3067-71.
17. Morimoto A, Oh Y, Nakamura S, Shioda Y, Hayase T, Imamura T, *et al.* Inflammatory serum cytokines and chemokines increase associated with the disease extent in pediatric Langerhans cell histiocytosis. Cytokine **2017**;97:73-9 doi 10.1016/j.cyto.2017.05.026.
18. Durham BH, Lopez-Rodrigo E, Abramson DH, Picarsic J, Pastore A, Mandelker D, *et al.* Activating Mutations in CSF1R and Additional Receptor Tyrosine Kinases in Sporadic and Familial Histiocytic Neoplasms. Blood **2018**;132(1):1 doi https://doi.org/10.1182/blood-2018-99-114248.
19. Martin-Moreno AM, Roncador G, Maestre L, Mata E, Jimenez S, Martinez-Torrecuadrada JL, *et al.* CSF1R Protein Expression in Reactive Lymphoid Tissues and Lymphoma: Its Relevance in Classical Hodgkin Lymphoma. PloS one **2015**;10(6):e0125203 doi 10.1371/journal.pone.0125203.
20. Vermi W, Bonecchi R, Facchetti F, Bianchi D, Sozzani S, Festa S, *et al.* Recruitment of immature plasmacytoid dendritic cells (plasmacytoid monocytes) and myeloid dendritic cells in primary cutaneous melanomas. The Journal of pathology **2003**;200(2):255-68 doi 10.1002/path.1344.
21. Milne P, Bigley V, Gunawan M, Haniffa M, Collin M. CD1c+ blood dendritic cells have Langerhans cell potential. Blood **2015**;125(3):470-3 doi 10.1182/blood-2014-08-593582.
22. Milne P, Bigley V, Bacon CM, Neel A, McGovern N, Bomken S, *et al.* Hematopoietic origin of Langerhans cell histiocytosis and Erdheim-Chester disease in adults. Blood **2017**;130(2):167-75 doi 10.1182/blood-2016-12-757823.
23. Collin M, Bigley V. Human dendritic cell subsets: an update. Immunology **2018**;154(1):3-20 doi 10.1111/imm.12888.
24. Kissenpfennig A, Henri S, Dubois B, Laplace-Builhe C, Perrin P, Romani N, *et al.* Dynamics and function of Langerhans cells in vivo: dermal dendritic cells colonize lymph node areas distinct from slower migrating Langerhans cells. Immunity **2005**;22(5):643-54 doi 10.1016/j.immuni.2005.04.004.
25. Boulakirba S, Pfeifer A, Mhaidly R, Obba S, Goulard M, Schmitt T, *et al.* IL-34 and CSF-1 display an equivalent macrophage differentiation ability but a different polarization potential. Scientific reports **2018**;8(1):256 doi 10.1038/s41598-017-18433-4.
26. El-Gamal MI, Anbar HS, Yoo KH, Oh CH. FMS Kinase Inhibitors: Current Status and Future Prospects. Medicinal research reviews **2013**;33(3):599-636 doi 10.1002/med.21258.
27. Jones GE, Prigmore E, Calvez R, Hogan C, Dunn GA, Hirsch E, *et al.* Requirement for PI 3-kinase gamma in macrophage migration to MCP-1 and CSF-1. Experimental cell research **2003**;290(1):120-31.
28. Stanley ER, Chitu V. CSF-1 receptor signaling in myeloid cells. Cold Spring Harbor perspectives in biology **2014**;6(6) doi 10.1101/cshperspect.a021857.
29. Mollah ZU, Aiba S, Nakagawa S, Hara M, Manome H, Mizuashi M, *et al.* Macrophage colony-stimulating factor in cooperation with transforming growth factor-beta1 induces the differentiation of CD34+ hematopoietic progenitor cells into Langerhans cells under serum-free conditions without granulocyte-macrophage colony-stimulating

factor. The Journal of investigative dermatology **2003**;120(2):256-65 doi 10.1046/j.1523-1747.2003.12036.x.

30. Strobl H, Bello-Fernandez C, Riedl E, Pickl WF, Majdic O, Lyman SD*, et al.* flt3 ligand in cooperation with transforming growth factor-beta1 potentiates in vitro development of Langerhans-type dendritic cells and allows single-cell dendritic cell cluster formation under serum-free conditions. Blood **1997**;90(4):1425-34.
31. Geissmann F, Lepelletier Y, Fraitag S, Valladeau J, Bodemer C, Debre M*, et al.* Differentiation of Langerhans cells in Langerhans cell histiocytosis. Blood **2001**;97(5):1241-8.
32. Martinez-Cingolani C, Grandclaudon M, Jeanmougin M, Jouve M, Zollinger R, Soumelis V. Human blood BDCA-1 dendritic cells differentiate into Langerhans-like cells with thymic stromal lymphopoietin and TGF-beta. Blood **2014**;124(15):2411-20 doi 10.1182/blood-2014-04-568311.
33. Wang Y, Bugatti M, Ulland TK, Vermi W, Gilfillan S, Colonna M. Nonredundant roles of keratinocyte-derived IL-34 and neutrophil-derived CSF1 in Langerhans cell renewal in the steady state and during inflammation. European journal of immunology **2016**;46(3):552-9 doi 10.1002/eji.201545917.
34. Hoshino N, Katayama N, Shibasaki T, Ohishi K, Nishioka J, Masuya M*, et al.* A novel role for Notch ligand Delta-1 as a regulator of human Langerhans cell development from blood monocytes. Journal of leukocyte biology **2005**;78(4):921-9 doi 10.1189/jlb.1204746.
35. Atmatzidis DH, Lambert WC, Lambert MW. Langerhans cell: exciting developments in health and disease. Journal of the European Academy of Dermatology and Venereology : JEADV **2017**;31(11):1817-24 doi 10.1111/jdv.14522.
36. Ries CH, Hoves S, Cannarile MA, Ruttinger D. CSF-1/CSF-1R targeting agents in clinical development for cancer therapy. Current opinion in pharmacology **2015**;23:45-51 doi 10.1016/j.coph.2015.05.008.
37. Takashima A, Edelbaum D, Kitajima T, Shadduck RK, Gilmore GL, Xu S*, et al.* Colony-stimulating factor-1 secreted by fibroblasts promotes the growth of dendritic cell lines (XS series) derived from murine epidermis. Journal of immunology **1995**;154(10):5128-35.
38. Caux C, Vanbervliet B, Massacrier C, Dezutter-Dambuyant C, de Saint-Vis B, Jacquet C*, et al.* CD34+ hematopoietic progenitors from human cord blood differentiate along two independent dendritic cell pathways in response to GM-CSF+TNF alpha. The Journal of experimental medicine **1996**;184(2):695-706.
39. Chomarat P, Banchereau J, Davoust J, Palucka AK. IL-6 switches the differentiation of monocytes from dendritic cells to macrophages. Nature immunology **2000**;1(6):510-4 doi 10.1038/82763.
40. Rohde CM, Schrum J, Lee AW. A juxtamembrane tyrosine in the colony stimulating factor-1 receptor regulates ligand-induced Src association, receptor kinase function, and down-regulation. The Journal of biological chemistry **2004**;279(42):43448-61 doi 10.1074/jbc.M314170200.
41. Xiong Y, Song D, Cai Y, Yu W, Yeung YG, Stanley ER. A CSF-1 receptor phosphotyrosine 559 signaling pathway regulates receptor ubiquitination and tyrosine phosphorylation. The Journal of biological chemistry **2011**;286(2):952-60 doi 10.1074/jbc.M110.166702.
42. Soares MJ, Pinto M, Henrique R, Vieira J, Cerveira N, Peixoto A*, et al.* CSF1R copy number changes, point mutations, and RNA and protein overexpression in renal cell carcinomas. Modern pathology : an official journal of the United States and Canadian Academy of Pathology, Inc **2009**;22(6):744-52 doi 10.1038/modpathol.2009.43.

43. Droin N, Solary E. Editorial: CSF1R, CSF-1, and IL-34, a "menage a trois" conserved across vertebrates. Journal of leukocyte biology **2010**;87(5):745-7 doi 10.1189/jlb.1209780.
44. Chihara T, Suzu S, Hassan R, Chutiwitoonchai N, Hiyoshi M, Motoyoshi K, *et al.* IL-34 and M-CSF share the receptor Fms but are not identical in biological activity and signal activation. Cell death and differentiation **2010**;17(12):1917-27 doi 10.1038/cdd.2010.60.
45. Pixley FJ, Stanley ER. CSF-1 regulation of the wandering macrophage: complexity in action. Trends in cell biology **2004**;14(11):628-38 doi 10.1016/j.tcb.2004.09.016.
46. Laoui D, Van Overmeire E, De Baetselier P, Van Ginderachter JA, Raes G. Functional Relationship between Tumor-Associated Macrophages and Macrophage Colony-Stimulating Factor as Contributors to Cancer Progression. Frontiers in immunology **2014**;5:489 doi 10.3389/fimmu.2014.00489.
47. West RB, Rubin BP, Miller MA, Subramanian S, Kaygusuz G, Montgomery K, *et al.* A landscape effect in tenosynovial giant-cell tumor from activation of CSF-1 expression by a translocation in a minority of tumor cells. Proceedings of the National Academy of Sciences of the United States of America **2006**;103(3):690-5 doi 10.1073/pnas.0507321103.
48. Carrera Silva EA, Nowak W, Tessone L, Olexen CM, Ortiz Wilczynski JM, Estecho IG, *et al.* CD207(+)CD1a(+) cells circulate in pediatric patients with active Langerhans cell histiocytosis. Blood **2017**;130(17):1898-902 doi 10.1182/blood-2017-05-782730.
49. Schwentner R, Jug G, Kauer MO, Schnoller T, Waidhofer-Sollner P, Holter W, *et al.* JAG2 signaling induces differentiation of CD14(+) monocytes into Langerhans cell histiocytosis-like cells. Journal of leukocyte biology **2019**;105(1):101-11 doi 10.1002/jlb.1a0318-098r.
50. Durham BH, Lopez Rodrigo E, Picarsic J, Abramson D, Rotemberg V, De Munck S, *et al.* Activating mutations in CSF1R and additional receptor tyrosine kinases in histiocytic neoplasms. Nature medicine **2019** doi 10.1038/s41591-019-0653-6.
51. Chakraborty R, Hampton OA, Shen X, Simko SJ, Shih A, Abhyankar H, *et al.* Mutually exclusive recurrent somatic mutations in MAP2K1 and BRAF support a central role for ERK activation in LCH pathogenesis. Blood **2014**;124(19):3007-15 doi 10.1182/blood-2014-05-577825.
52. Haroche J, Cohen-Aubart F, Emile JF, Maksud P, Drier A, Toledano D, *et al.* Reproducible and sustained efficacy of targeted therapy with vemurafenib in patients with BRAF(V600E)-mutated Erdheim-Chester disease. Journal of clinical oncology : official journal of the American Society of Clinical Oncology **2015**;33(5):411-8 doi 10.1200/JCO.2014.57.1950.
53. Diamond EL, Subbiah V, Lockhart AC, Blay JY, Puzanov I, Chau I, *et al.* Vemurafenib for BRAF V600-Mutant Erdheim-Chester Disease and Langerhans Cell Histiocytosis: Analysis of Data From the Histology-Independent, Phase 2, Open-label VE-BASKET Study. JAMA oncology **2018**;4(3):384-8 doi 10.1001/jamaoncol.2017.5029.
54. Azorsa DO, Lee DW, Wai DH, Bista R, Patel AR, Aleem E, *et al.* Clinical resistance associated with a novel MAP2K1 mutation in a patient with Langerhans cell histiocytosis. Pediatric blood & cancer **2018**;65(9):e27237 doi 10.1002/pbc.27237.
55. Gandolfi L, Adamo S, Pileri A, Broccoli A, Argnani L, Zinzani PL. Multisystemic and Multiresistant Langerhans Cell Histiocytosis: A Case Treated With BRAF Inhibitor. Journal of the National Comprehensive Cancer Network : JNCCN **2015**;13(6):715-8 doi 10.6004/jnccn.2015.0086.
56. Donadieu J, Larabi IA, Tardieu M, Visser J, Hutter C, Sieni E, *et al.* Vemurafenib for Refractory Multisystem Langerhans Cell Histiocytosis in Children: An International

Observational Study. Journal of clinical oncology : official journal of the American Society of Clinical Oncology **2019**;37(31):2857-65 doi 10.1200/jco.19.00456.

57. Giricz O, Mo Y, Dahlman KB, Cotto-Rios XM, Vardabasso C, Nguyen H*, et al.* The RUNX1/IL-34/CSF-1R axis is an autocrinally regulated modulator of resistance to BRAF-V600E inhibition in melanoma. JCI insight **2018**;3(14) doi 10.1172/jci.insight.120422.
58. Ngiow SF, Meeth KM, Stannard K, Barkauskas DS, Bollag G, Bosenberg M*, et al.* Co-inhibition of colony stimulating factor-1 receptor and BRAF oncogene in mouse models of BRAF(V600E) melanoma. Oncoimmunology **2016**;5(3):e1089381 doi 10.1080/2162402x.2015.1089381.

FIGURE LEGENDS

Figure 1: CSF1R recognizes CD207$^+$ LCs but not dermal CD207$^+$ DCs. Sections are from reactive human lung (**A**), esophagus (**B**), and skin (**C-I**) and stained as labeled. CD207$^+$ LCs in bronchus epithelium (**A**), esophagus mucosa (**B**) as well as normal skin (**C**) coexpress CSF1R. Dermal CSF1R$^+$ cells largely correspond to CD163$^+$ macrophages (**D**). CSF1R is mainly negative in CD207$^+$ (**E**), CD1a$^+$ (**F**), and BDCA1$^+$ (**G**) dermal DCs. Dermal CD207$^+$ DCs are mostly BDCA1$^+$ (**H**) and IRF4$^+$ (**I**). Green traces separate epidermis from dermis. Sections are counterstained with hematoxylin. Original Magnification: 200x (A, B, F; scale bar = 100 microns), 400x (C, D, G, I; scale bar = 50 microns) and 600x (E, H; scale bar 33 microns). Insets were obtained by single cell resizing of a 200x magnification. Micro-photographs were taken using the acquisition software cellSens (Olympus) and DP-73 Olympus digital camera mounted on the Olympus BX60 microscope.

Figure 2: Expression of CSF1R on human epidermal subpopulations. (**A**) Single cell suspensions from human epidermis were processed for flow cytometry analysis. Gating strategy used to exclude cell debris, doublets and dead cells is presented in the panel. CSF1R surface expression was analyzed in the CD1a$^+$CD207$^+$ fraction within the CD45$^+$ HLA-DR^{++} population (red). In parallel, expression of CSF1R was verified in CD45$^-$ (pink) and CD45$^+$ (yellow) cells. Fluorescence minus one (FMO) controls for the antibodies are shown. Data from one representative experiment are presented (n = 5). (**B**) CD45$^+$ epidermal cells were untreated or stimulated for 48 h with LPS (1 µg/ml) and R848 (5 µg/ml) and evaluated for CSF1R and CD83 expression by flow cytometry analysis, using the same gating strategy of panel A (one representative experiment out of four is shown). The values in the bottom graph show the average percentage of CSF1R$^+$ cells ± SEM from 4 independent experiments. * $p < 0.05$ vs. untreated cells by Student *t* test.

Figure 3: CSF1R modulation during DC differentiation and maturation. (**A**) LCs differentiated from human CD14$^+$ cells (mo-LCs), BDCA1$^+$ cells, and CD34$^+$ cells were evaluated for the expression of CSF1R in the CD1a$^+$CD207$^+$ fraction. Controls for CSF1R (fluorescence minus one, FMO) are shown. Representative flow cytometry analysis (top) and summary results (bottom; mean ± SEM) of respectively 6 (mo-LCs), 5 (BDCA1$^+$ LCs) and 4 (CD34$^+$ LCs) experiments are shown. (**B**) mo-LC were untreated or stimulated for 48 h with LPS (100 ng/ml) and R848 (1 ug/ml) and evaluated for CSF1R, CD83, and IRF4 expression by FACS analysis (one representative experiment is shown). FMO controls for all antibodies are shown. The values in the bottom graph show the average percentage of CSF1R$^+$ cells ± SEM evaluated in 4 independent experiments. * $p<0.05$ vs. untreated LCs by Student *t* test. Sections are from three human skin-draining lymph nodes with dermatopathic reaction and stained as labeled. CSF1R$^+$ cells are predominantly located at the periphery of dermatopathic CD1a$^+$ nodules (**C**) and within the lymphatic sinus coexpressing CD207 (**D** black arrows, **E**) but not IRF4 (**F**); sinuses are lined by PDPN$^+$ endothelial cells (**E**). Paracortical IDC nodules are composed by mature CD208$^+$CD207$^+$ IDC coexpressing IRF4 (**G**). The two IDC populations include CD207$^{+/-}$BDCA1$^+$ cells mainly in the outer paracortex and CD207$^+$BDCA1$^-$ in the inner paracortex (**H**); both populations express IRF4 (**H**). Sections are counterstained with hematoxylin. Original Magnification: 100x (C, D; scale bar = 200 micron), 200x (E, H: scale bar = 100 microns) and 600x (F, G; scale bar = 33 micron).

Figure 4. Effect of CSF1R ligands on LCs. (**A**) mo-LCs (2.5×10^5) were seeded in the upper compartments of a 24-well Transwell cell culture chamber; CSF-1 or IL34 (50 ng/ml) were added to the lower compartments. Cells that migrated to the lower compartments after 4 h incubation were counted by flow cytometry (left panel). Mo-LCs were preincubated with GW2580 (1uM) or BLZ945 (0.5 µM) for 1 h at 37°C. Thereafter, chemotaxis was measured in response to CSF-1 (mid

panel). The chemotaxis of BDCA1$^+$ LCs was measured in response to CSF-1 (50ng/ml) after 6 h incubation (right panel). Assays were performed in triplicate. Mean value ± SEM of 4 independent experiments for mo-LC and of 3 independent experiments for BDCA1$^+$ LCs are shown. * $p<0.05$ vs. untreated LCs; # $p<0.05$ vs. CSF1-migrated LCs by one-way ANOVA followed by Tukey's Multiple Comparison Test or by Student *t* test as appropriate. (**B**) LCs were differentiated from CD34$^+$ cells in presence of CSF-1 or GM-CSF for 14 and 10 days, respectively. In parallel, cells were treated with BLZ945 (0.5 uM) for the indicated culture conditions. One representative experiment of the expression of CD1a and CD207 is shown as a flow cytometry dot plot. Fluorescence minus one (FMO) controls for antibodies are shown. The average percentage of CD1a$^-$/CD207$^-$, CD1a$^+$/CD207$^-$ and CD1a$^+$/CD207$^+$ cells within CSF1-differentiated LCs and GM-CSF-differentiated LCs in presence or absence of BLZ945 is reported (mean value ± SEM of 3 independent experiments) * $p<0.05$ vs. untreated LCs by Student *t* test.

Figure 5: CSF1R expression in LCH. Sections are from 5 human LHC and stained as labeled. Phenotypical characterization of two LCH (**A-T**), *BRAF*^{V600} (**A-J**) and *BRAF*^{V600E} (**K-T**) as defined by VE1 stain and digital PCR. Neoplastic cells, recognized by double stain for VE1 and CD207 (**U**) coexpress CSF1R (**V, W**). In the LCH microenvironment, CSF1R is also expressed on CD163$^+$ macrophages (**X**). A representative LCH case showing coexpression of CD207$^+$ and IRF4$^+$ in neoplastic cells is reported in **Y**. Sections are counterstained with hematoxylin. Original Magnification: 40x (A-E, K-O; scale bar = 500 micron), 400x (F-J, P-T, U, V, X, Y; scale bar = 50 microns) and 600x (W; scale bar = 33 µm).

Figure 6: CSF1R, CSF1, IL34 mRNA, and phospho-p44/42 MAPK (Thr202/Tyr204) in LCH tissue. The graphs illustrate the ddPCR-based detection of mRNA of KRT14, CD207, and CSF1R (**A**), as well as CSF-1 and IL34 (**B**) in 12 LCH samples from cutaneous (n = 7) and extracutaneous (n = 5) sites. All samples were normalized to UBC mRNA expression. Undetectable mRNA are reported as 0.01. Sections are from two *BRAF* wild-type LCH cases (#8 C-E, #36 F-H) and stained as labelled. On serial sections, LCH cells stained for anti–phospho-p44/42 MAPK (Thr202/Tyr204) (**C, D and F, G**); the latter marker is also observed in a fraction of surrounding tumor-associated macrophages (**E and H**) as documented by staining for CD163. Sections are counterstained with hematoxylin. Original Magnification: 200x (**C**, **D**, **F** and **G; scale bar 100 µm**) and 400x (**E** and **H; scale bar 50 µm**).

FIGURE 1

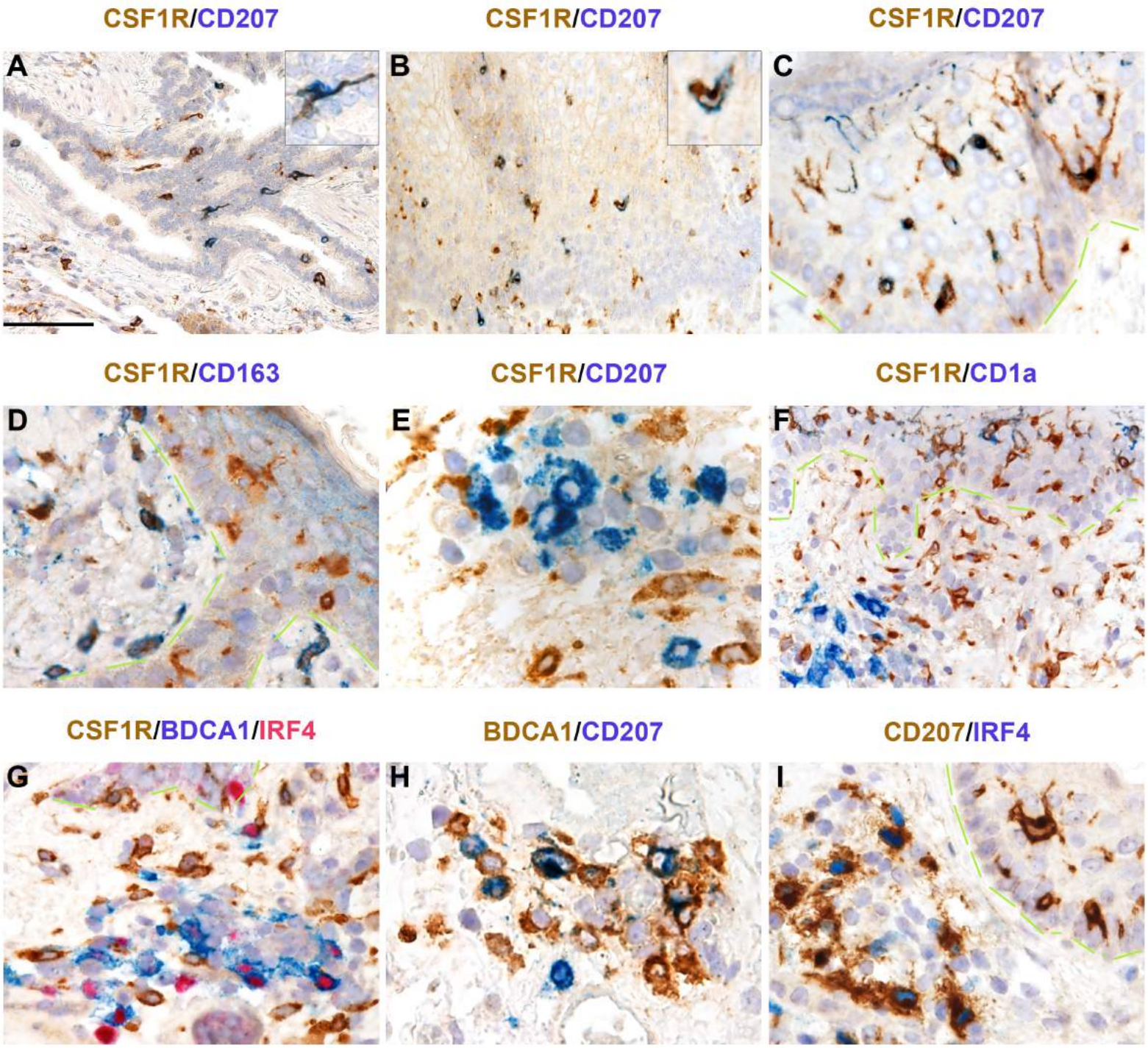
CSF1R/CD207
A
CSF1R/CD207
B
CSF1R/CD207
C
CSF1R/CD163
D
CSF1R/CD207
E
CSF1R/CD1a
F
CSF1R/BDCA1/IRF4
G
BDCA1/CD207
H
CD207/IRF4
I

FIGURE 2

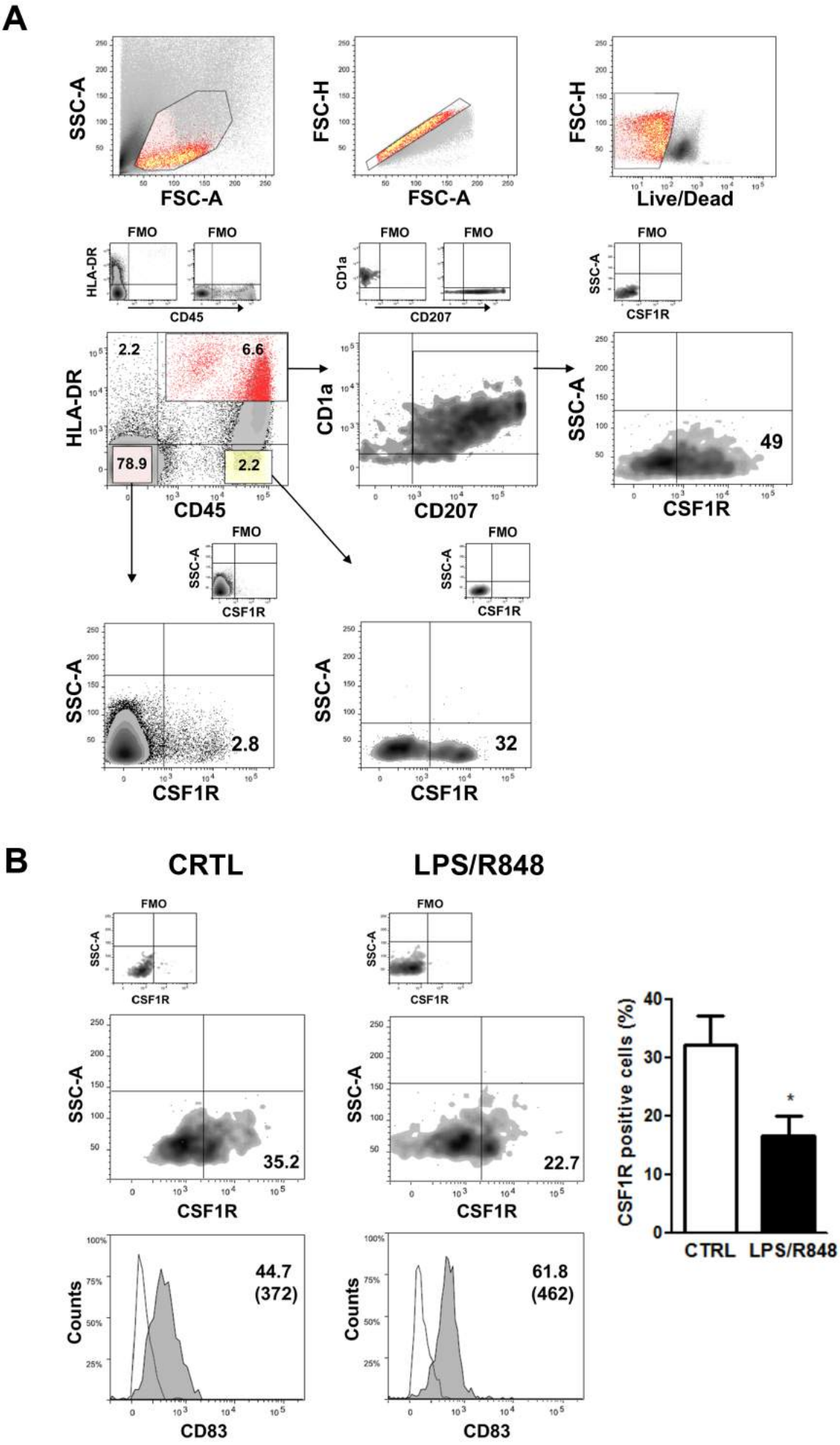
A
SSC-A
FSC-A
FSC-H
FSC-A
FSC-H
Live/Dead
FMO
FMO
HLA-DR
CD45
FMO
FMO
CD1a
CD207
FMO
SSC-A
CSF1R
2.2
6.6
78.9
2.2
HLA-DR
CD45
CD1a
CD207
SSC-A
49
CSF1R
FMO
SSC-A
CSF1R
FMO
SSC-A
CSF1R
SSC-A
2.8
CSF1R
SSC-A
32
CSF1R
B
CRTL
LPS/R848
FMO
SSC-A
CSF1R
FMO
SSC-A
CSF1R
SSC-A
35.2
CSF1R
SSC-A
22.7
CSF1R
Counts
44.7
(372)
CD83
Counts
61.8
(462)
CD83
CSF1R positive cells (%)
40
30
20
10
0
*
CTRL
LPS/R848

FIGURE 3

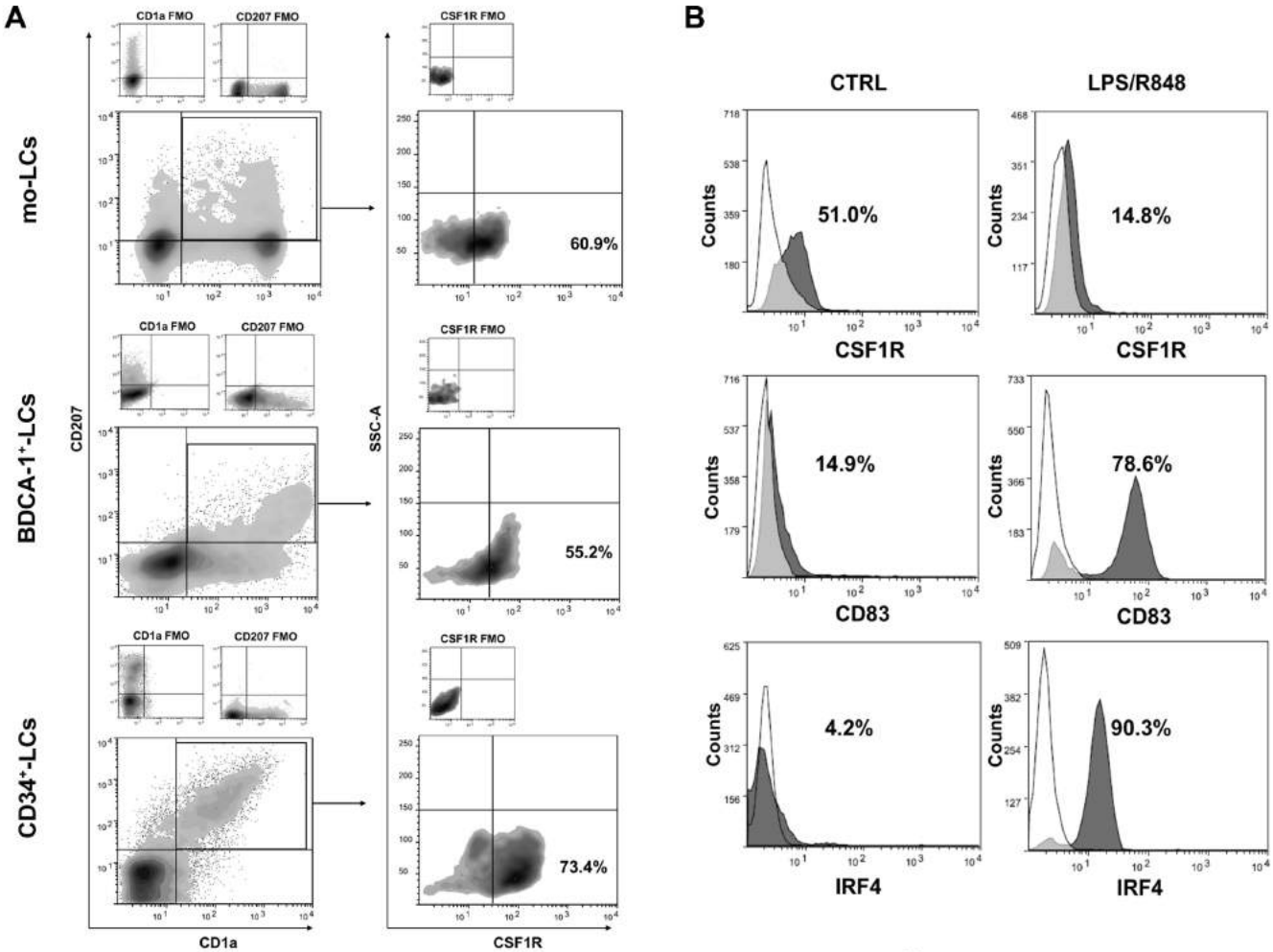
A
CD1a FMO
CD207 FMO
CSF1R FMO
mo-LCs
BDCA-1+-LCs
CD34+-LCs
CD207
SSC-A
CD1a
CSF1R
60.9%
55.2%
73.4%
B
CTRL
LPS/R848
Counts
51.0%
14.8%
14.9%
78.6%
4.2%
90.3%
CSF1R
CD83
IRF4

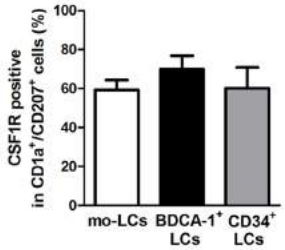
CSF1R positive in CD1a+/CD207+ cells (%)
mo-LCs
BDCA-1+ LCs
CD34+ LCs

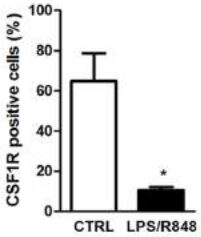
CSF1R positive cells (%)
CTRL
LPS/R848
*

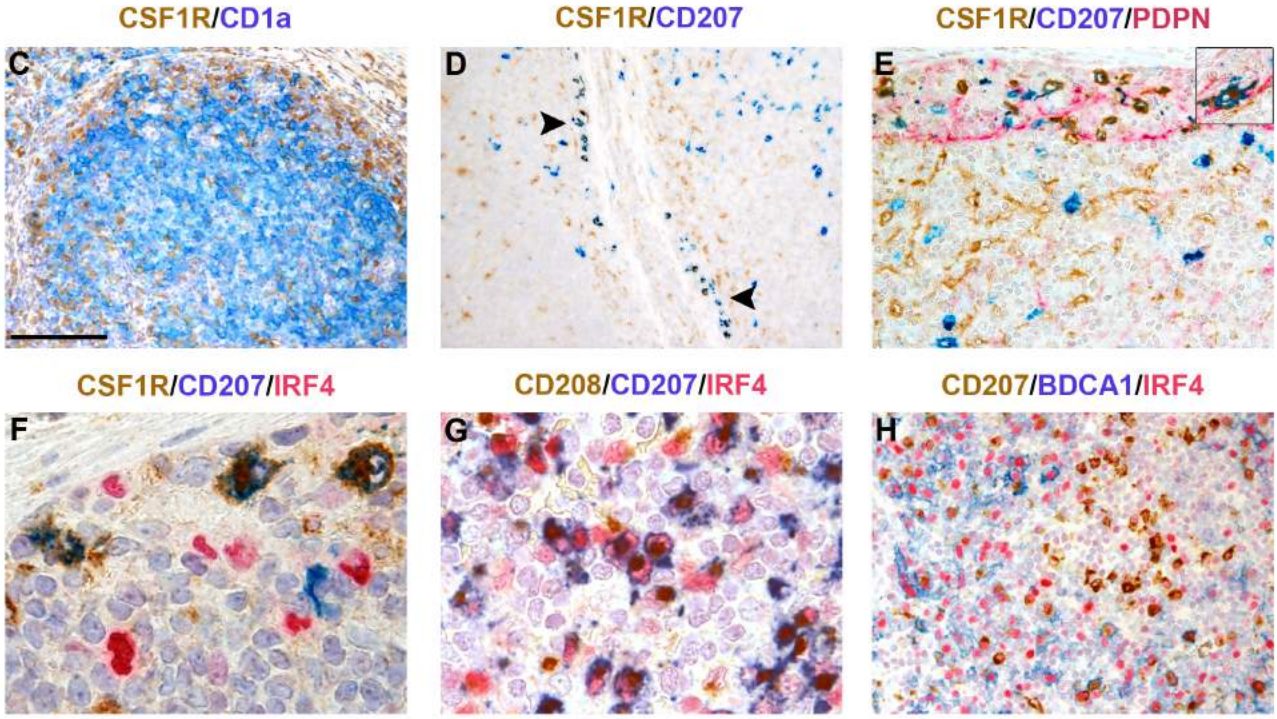
CSF1R/CD1a
C
CSF1R/CD207
D
CSF1R/CD207/PDPN
E
CSF1R/CD207/IRF4
F
CD208/CD207/IRF4
G
CD207/BDCA1/IRF4
H

FIGURE 4

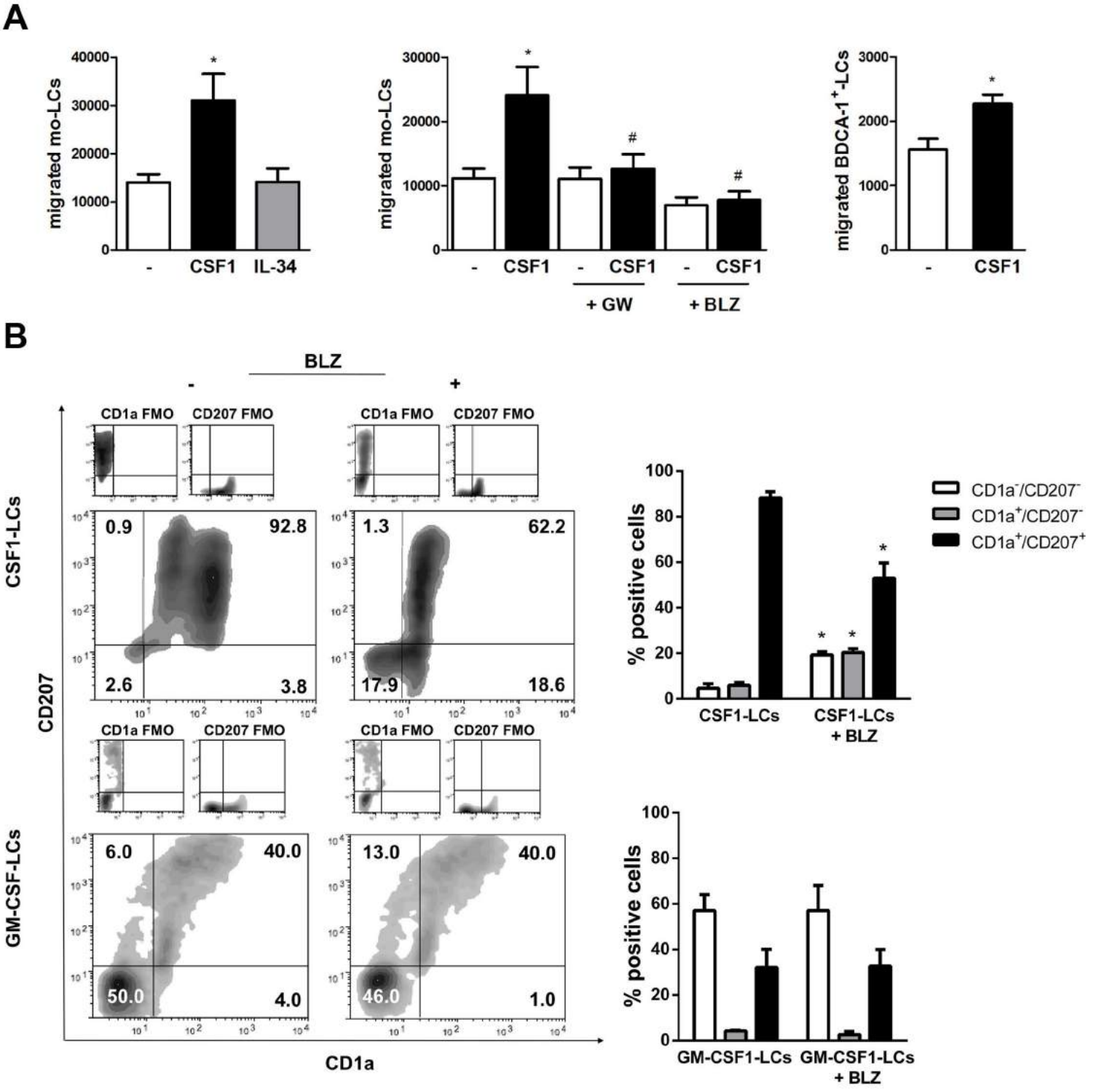
A
migrated mo-LCs
40000
30000
20000
10000
0
*
-
CSF1
IL-34
migrated mo-LCs
30000
20000
10000
0
*
#
#
-
CSF1
-
CSF1
-
CSF1
+ GW
+ BLZ
migrated BDCA-1+-LCs
3000
2000
1000
0
*
-
CSF1
B
BLZ
-
+
CD1a FMO
CD207 FMO
CD1a FMO
CD207 FMO
CSF1-LCs
0.9
92.8
2.6
3.8
1.3
62.2
17.9
18.6
CD207
CD1a FMO
CD207 FMO
CD1a FMO
CD207 FMO
GM-CSF-LCs
6.0
40.0
50.0
4.0
13.0
40.0
46.0
1.0
CD1a
% positive cells
100
80
60
40
20
0
CD1a-/CD207-
CD1a+/CD207-
CD1a+/CD207+
*
*
*
CSF1-LCs
CSF1-LCs
+ BLZ
% positive cells
100
80
60
40
20
0
GM-CSF1-LCs
GM-CSF1-LCs
+ BLZ

FIGURE 5

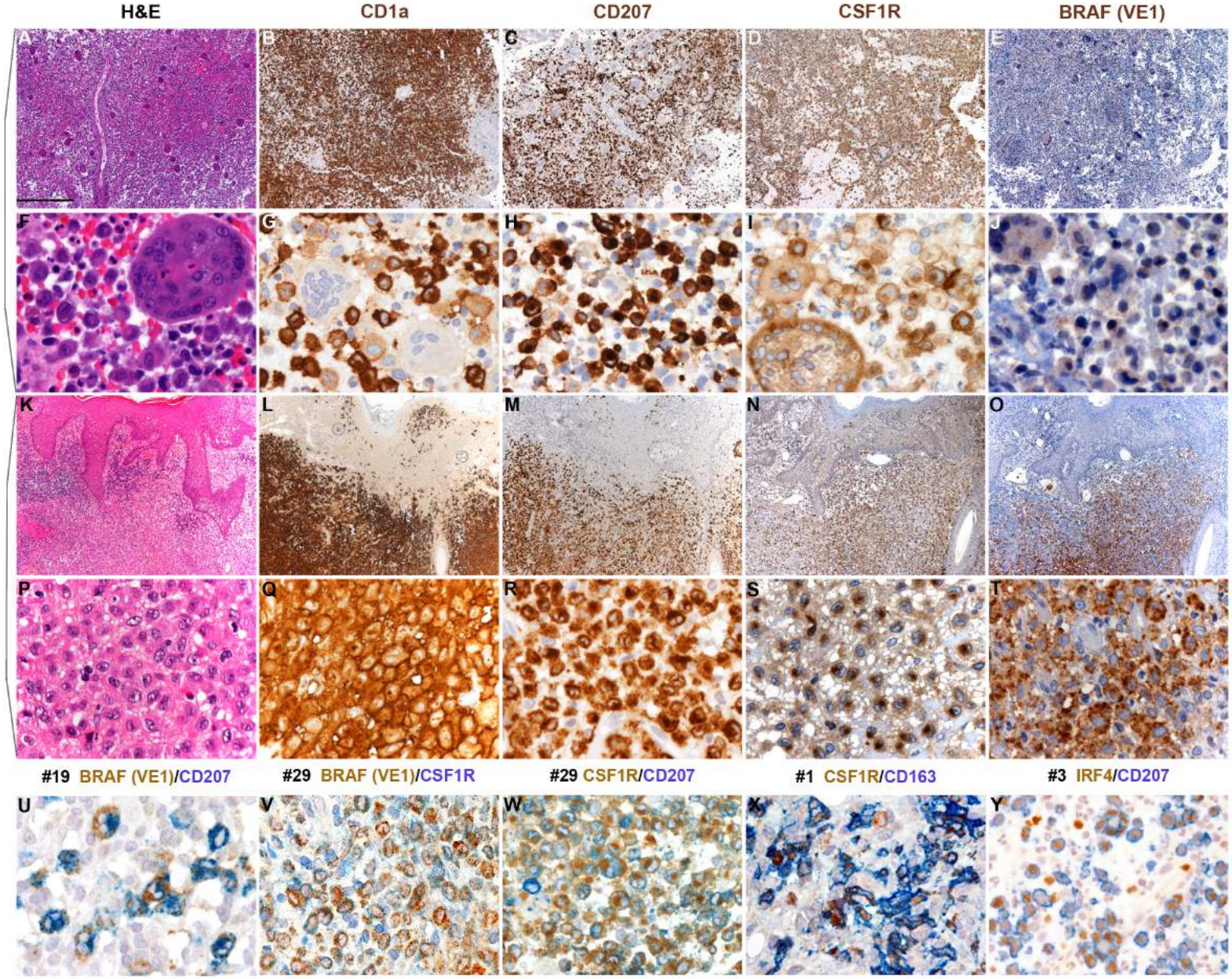
H&E
CD1a
CD207
CSF1R
BRAF (VE1)
#8
#1
A
B
C
D
E
F
G
H
I
J
K
L
M
N
O
P
Q
R
S
T
#19 BRAF (VE1)/CD207
#29 BRAF (VE1)/CSF1R
#29 CSF1R/CD207
#1 CSF1R/CD163
#3 IRF4/CD207
U
V
W
X
Y

FIGURE 6

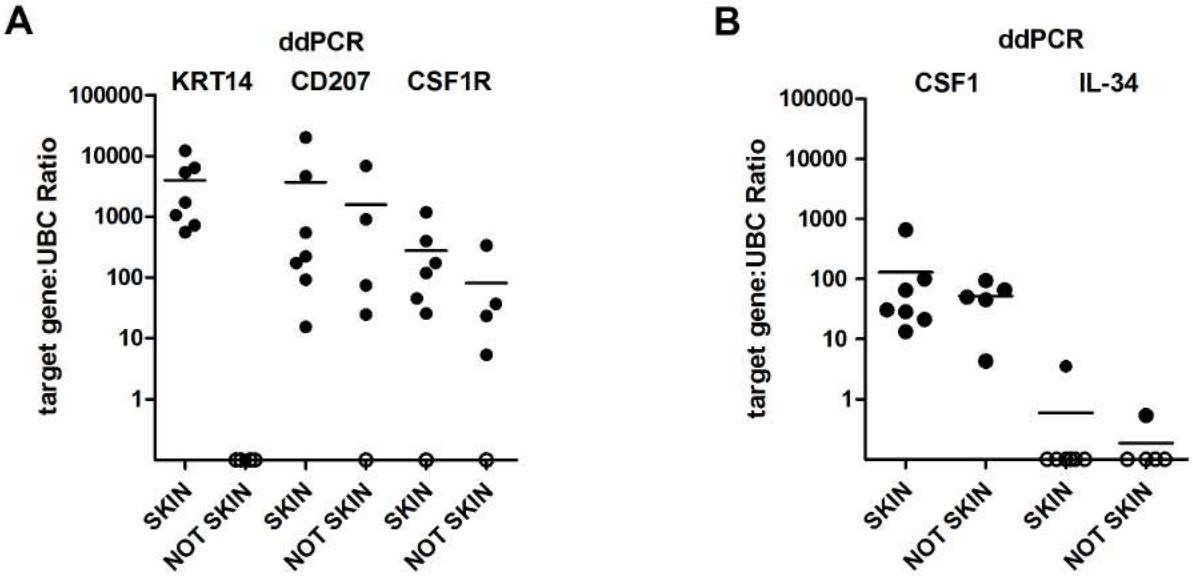
A
ddPCR
KRT14
CD207
CSF1R
target gene:UBC Ratio
100000
10000
1000
100
10
1
SKIN
NOT SKIN
SKIN
NOT SKIN
SKIN
NOT SKIN
B
ddPCR
CSF1
IL-34
target gene:UBC Ratio
100000
10000
1000
100
10
1
SKIN
NOT SKIN
SKIN
NOT SKIN

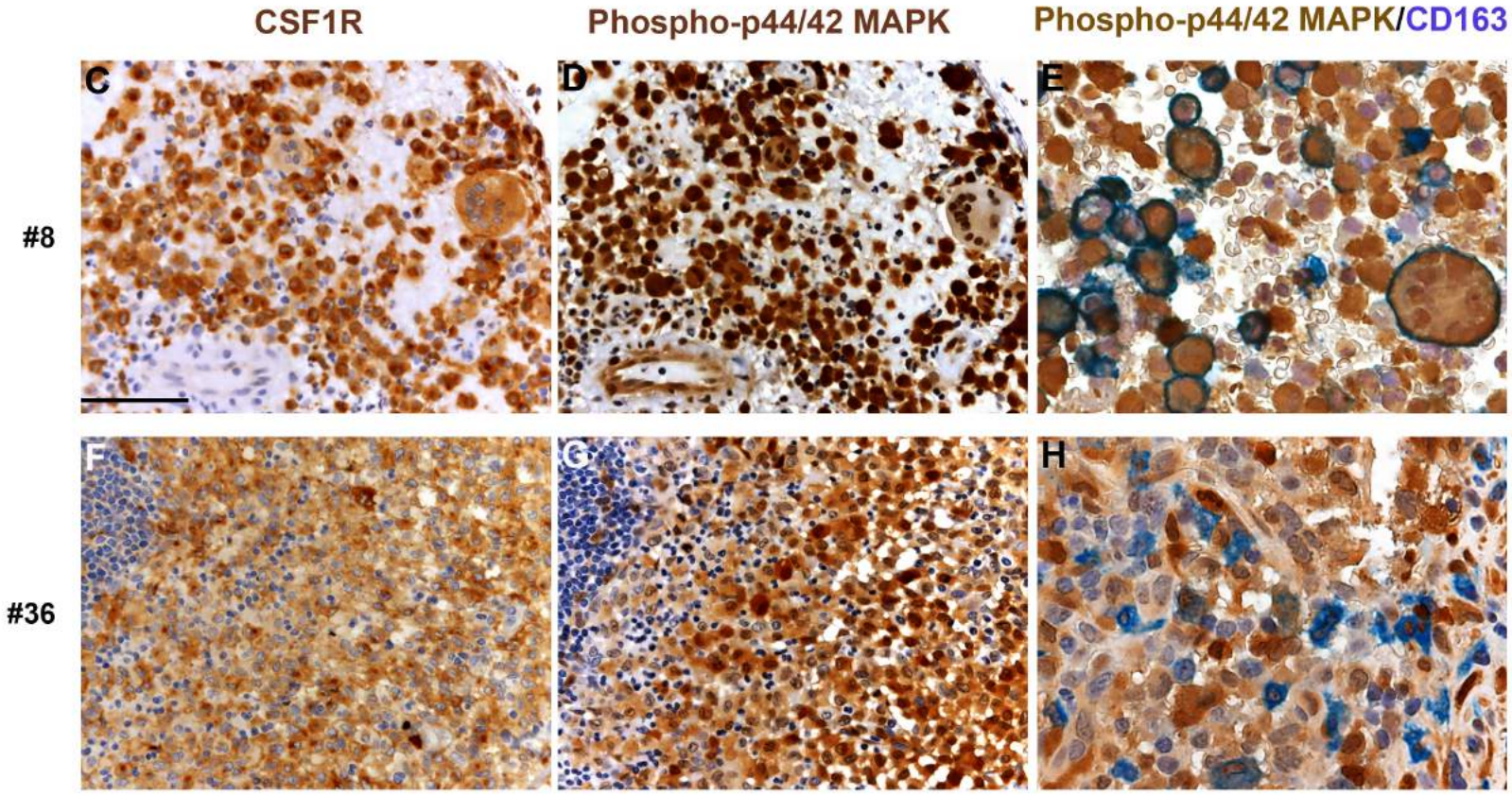
CSF1R
Phospho-p44/42 MAPK
Phospho-p44/42 MAPK/CD163
#8
#36
C
D
E
F
G
H